International Journal of Mass Spectrometry 429 (2018) 121–126

Contents lists available at ScienceDirect

International Journal of Mass Spectrometry

journal homepage: www.elsevier.com/locate/ijms

Mass-resolved ion microscope imaging over expanded mass ranges using double-field post-extraction differential acceleration

Ang Guo, Michael Burt, Mark Brouard *

The Department of Chemistry, University of Oxford, The Chemistry Research Laboratory, 12 Mansfield Road, Oxford OX1 3TA, United Kingdom

ARTICLE INFO

Article history:
Received 15 February 2017
Received in revised form 8 June 2017
Accepted 22 June 2017
Available online 3 July 2017

Keywords:
Mass spectrometry imaging
Post extraction differential acceleration (PEDA)
Spatial-map imaging
Ion optics

ABSTRACT

A modified post-extraction differential acceleration (PEDA) technique employing two pulsed electrodes was used to demonstrate mass-resolved stigmatic imaging over a broad m/z range. By varying the pulse voltages, a potential energy cusp was introduced into the ion acceleration region of an imaging mass spectrometer, creating two m/z foci that were tuned to overlap at the detector plane. This resulted in two focused m/z distributions that stretched the mass-resolved window with $m/\Delta m \geq 1000$ to 165 Da without any loss in image quality; a range that doubled the 65 Da achieved under similar conditions using the original PEDA technique.

1. Introduction

Mass spectrometry imaging (MSI) is widely used to obtain mass-specific surface images with micron or sub-micron spatial resolutions [1–4]. Since its maturation in the late 1990s, MSI has frequently been coupled with matrix-assisted laser desorption ionization (MALDI) [5], secondary ion mass spectrometry (SIMS) [6], and desorption electrospray ionization (DESI) [7] to generate and image ions from a wide range of samples. This has led to its uptake in omics-based life sciences, where it has been applied to image polymers, metabolites, and other biomarkers [8–13].

Imaging mass spectrometers are typically microprobe instruments where a focused laser, ion beam, or electrospray source is used to desorb and ionize molecules at a surface spot. Mass spectra are recorded with their locations by raster scanning the ionizing probe across the surface, enabling ion images to be reconstructed by plotting the intensity of specific ions at different probe positions. Like other scanning imaging techniques, such as electron microscopy [14], the spatial resolution of MSI is determined by the probe spot size. The drawback of this approach is that the time required to collect an image is inversely proportional to the area of the probe beam.

Microscope MSI has the potential to record spatially-resolved ion images faster than microprobe methods. In this approach, sample surfaces are illuminated with a defocused laser or ion beam, enabling all surface molecules to be desorbed and ionized simultaneously [15–17]. The spatial distribution of ions is then electrostatically projected onto a position-sensitive imaging detector at the end of a time-of-flight mass analyzer. This process is analogous to stigmatic microscopy, and has the advantage of decoupling spatial resolution from the probe beam size while retaining resolutions of 1–20 μm.

Although the principles of ion microscopy have been well established since the 1960s [18], their uptake compared to microprobe instruments has been limited due to the difficulty in imaging more than one m/z (or range of m/z) during an experimental cycle. The advent of event-triggered sensors, such as CMOS-based cameras [19–21], has overcome this problem by removing the need to apply time gates to the detector; ion images can now be recorded for every resolved m/z in a defined mass range during a single experiment [22–24].

The challenge in microscope MSI has therefore shifted from multi-mass imaging to the simultaneous optimization of mass and spatial resolution over a broad mass range. These are limited by the initial distribution of ion velocities at the sample surface. Mass resolution can be corrected using delayed extraction [25–28], but the spatial resolution will remain poor as nothing prevents ions from diffusing away from their initial time-of-flight axes. Aoki and coworkers resolved this by developing the post extraction differential acceleration (PEDA) method [29], which extracts ions from a surface immediately following ionization to preserve their spatial resolution. Initial velocity distributions are then corrected by rais-

* Corresponding author.
E-mail address: mark.brouard@chem.ox.ac.uk (M. Brouard).

https://doi.org/10.1016/j.ijms.2017.06.010
1387-3806/

ing the potential of the extraction electrode after the ion packet has passed it. This causes slower ions of a particular m/z to accumulate more kinetic energy than quicker ions, creating a temporal focal point that is tuned to correspond with the detector plane. Using this approach, mass and spatial resolutions of 1450 $m/\Delta m$ and 4.0–5.5 μm were simultaneously achieved. PEDA has since been applied over wide mass ranges using velocity corrected ion extraction [30], where the applied extraction field is retuned to shift the PEDA window to different m/z ranges without changing the image magnification or the mass and spatial resolutions.

This report describes an improved PEDA variant that uses an additional electrode to broaden the resolved mass window. The following sections introduce this 'double-field' PEDA concept, and experimentally compare it with the single-field method.

2. Theory and simulations

In single-field PEDA, lighter ions have earlier temporal focal points than heavier ions. As the field free drift length is fixed, ion optical voltages must therefore be tuned to focus a particular m/z, and the effective mass range is consequently centered around this focal point. The temporal foci of two m/z can be made to overlap by introducing a second pulsed electrode to the PEDA acceleration region. This double-field PEDA method is illustrated in Fig. 1, where an additional electrode is inserted midway between the extractor and einzel lens entrance. The raised potentials of the two pulsed electrodes are used to create a cusp in the potential surface that divides the acceleration region in two. When the pulse applied to the new plate is less than half of that applied to the extractor, heavier ions in the 'early' acceleration region pass through a larger acceleration field than lighter ions in the 'late' region. By adjusting the potential energy gradient on each side of the added electrode, an m/z from each segment of the acceleration region can be simultaneously focused, thereby broadening the achievable mass range. In the present work, the position of the added electrode and its applied pulse voltage are used to establish, at minimum, a 1000 $m/\Delta m$ resolution over the mass range between the two focused m/z. As these foci are governed by the electric fields in the 'early' and 'late' acceleration regions, it should be noted that the same effect can in principle be duplicated by repositioning the PEDA electrode within the acceleration region and modifying the pulse voltage.

Following Aoki and coworkers, the extraction region in Fig. 1 is defined with length L_1 and potential difference V_E [29]. An ion with mass m, charge q, and initial velocity v_0 extracted from the charged surface at $x=0$ will therefore accelerate to v_1 when it reaches the extractor electrode at $x=L_1$. The flight time over this region is described by t_1:

$$v_1 = \sqrt{\frac{2}{m}\left(\frac{mv_0^2}{2} + qV_E\right)} \tag{1}$$

$$t_1 = \frac{mv_0L_1}{qV_E}\left(-1 + \sqrt{1 + \frac{2qV_E}{mv_0^2}}\right) \tag{2}$$

The ion then enters an acceleration region between the extractor electrode and einzel lens entrance with potential difference V_A and length L_2. The additional PEDA electrode is placed at $x=L_1+L_2/2$ with potential $V_A/2$. At a set time τ, the extractor and PEDA electrodes are raised by ΔV_{A1} and ΔV_{A2}, respectively. When these pulses are applied, the ion is located at $x=L_1+L_p$ with a velocity v_p. These are given by:

$$L_p = v_1(\tau - t_1) + \frac{qV_A}{2mL_2}(\tau - t_1)^2 \tag{3}$$

$$v_p = \sqrt{\frac{2}{m}\left(\frac{1}{2}mv_0^2 + q\left(V_E + V_A\frac{L_p}{L_2}\right)\right)} \tag{4}$$

At τ, ions located in the 'early' and 'late' acceleration region will accelerate differently. For ions at $L_p \geq L_2/2$, the potential increase resulting from the pulsed electrodes is the same as in the original PEDA case.

$$\Delta V = 2\Delta V_{A2}\left(1 - \frac{L_p}{L_2}\right) \tag{5}$$

The potential change for ions at $L_p < L_2/2$ is similar to the above, but accounts for the difference between ΔV_{A1} and ΔV_{A2}.

$$\Delta V = \Delta V_{A2} + (\Delta V_{A1} - \Delta V_{A2})\left(1 - \frac{L_p}{L_2/2}\right) \tag{6}$$

In both cases, the velocity of the ion as it leaves the acceleration region, v_2, is given by substituting the appropriate ΔV into the following equation:

$$v_2 = \sqrt{\frac{2}{m}\left[\frac{mv_0^2}{2} + q(V_E + V_A + \Delta V)\right]} \tag{7}$$

The time at which the ion leaves the acceleration region also depends on its position. When $L_p \geq L_2/2$, the ion flight time at the einzel lens entrance, t_2, is:

$$t_2 = \tau + \frac{mv_p}{qE_2}\left[-1 + \sqrt{1 + \frac{qE_2\left(L_2 - L_p\right)}{mv_p^2/2}}\right] \tag{8}$$

To calculate t_2 when $L_p < L_2/2$, the ion velocity and time-of-flight at the additional PEDA electrode, v_m and t_m, must be determined. In the following, E_1 and E_2 are the electric field strengths of the 'early' and 'late' acceleration region, and are defined as $\{2(\Delta V_{A1} - \Delta V_{A2}) + V_A\}/L_2$ and $(2\Delta V_{A2} + V_A)/L_2$:

$$t_2 = t_m + \frac{mv_m}{qE_2}\left(-1 + \sqrt{1 + \frac{qE_2L_2}{mv_m^2}}\right) \tag{9}$$

$$v_m = \sqrt{\frac{2}{m}\left(\frac{1}{2}mv_p^2 + qE_1\left(L_2/2 - L_p\right)\right)} \tag{10}$$

$$t_m = \tau + \frac{mv_p}{qE_1}\left(-1 + \sqrt{1 + \frac{qE_1\left(L_2/2 - L_p\right)}{mv_p^2/2}}\right) \tag{11}$$

At this stage, the ion enters a conventional three-electrode einzel lens with a grounded entrance and exit. Each lens electrode is separated by a length L_3. The ion leaves the einzel lens at time t_3 with

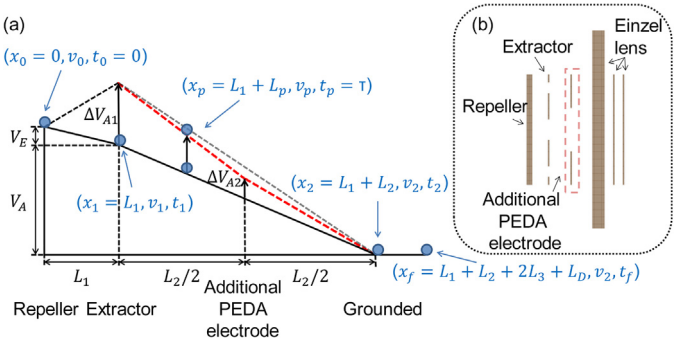

Fig. 1. (a) The electrode potential energy surface (black line) before and after the application of single-field (black dashed line) and double-field PEDA (red dashed line). In the double-field case, heavier ions in the 'early' acceleration region (L_1 to $L_1+L_2/2$) experience a larger acceleration field than lighter ions in the 'late' region ($L_1+L_2/2$ to L_1+L_2), creating two focal points that are tuned to overlap at the detector. (b) The instrument ion optics used for single- and double-field PEDA.